JPET-AR-2020-000235

Interaction of halogenated tyrosine/phenylalanine-derivatives with Organic Anion Transporter (OAT) 1 in the renal handling of tumor imaging probes

Chunhuan Jin, Ling Wei, Ryuichi Ohgaki, Hideyuki Tominaga, Minhui Xu, Suguru Okuda, Hiroki Okanishi, Yasuharu Kawamoto, Xin He, Shushi Nagamori, and Yoshikatsu Kanai

Journal of Pharmacology and Experimental Therapeutics (JPET)

Supplemental Figure 1

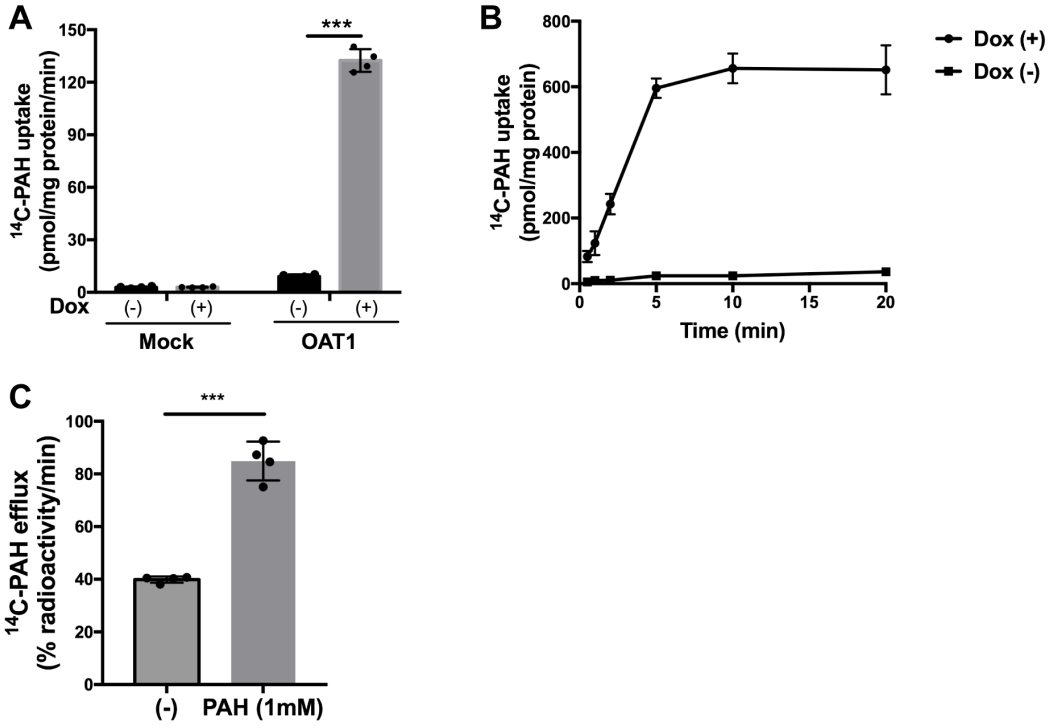

Supplemental Figure 1. Functional characterization of FlpIn293-TetR-hOAT1 cell line.

(A) ^{14}C-PAH uptake in FlpIn293-TetR-hOAT1 cells. Uptake of 1μM ^{14}C-PAH was measured for 1 min in the Mock cells or FlpIn293-TetR-hOAT1 cells ("OAT1") treated with (+) or without (−) doxycycline ("Dox"). Mock cells are the Flp-In T-Rex-293 cells transfected with pcDNA5/FRT/TO vector without OAT1 cDNA insert (see text). Data represent means ± SD, n = 4. *** $p < 0.001$. $p = 0.0004$. ***(B)*** Time course of ^{14}C-PAH uptake. The uptake of ^{14}C-PAH (1 μM) was measured up to 20 min in FlpIn293-TetR-hOAT1 cells with (+) or without (−) treatment with doxycycline ("Dox"). Data

represent means ± SD, n = 4. ***(C)*** ^{14}C-PAH efflux induced by PAH in OAT1 cells. OAT1 cells were preloaded with ^{14}C-PAH as described in "Materials and Methods". After washing, the cells were incubated for 1 min in the presence or absence (−) of 1mM extracellular PAH. The radioactivity in the medium regarded as the efflux was expressed as the percent of total preloaded radioactivity (see text). *** $p < 0.001$ vs. (−). $p = 0.0007$. Data are expressed as means ± SD (n=4). In each efflux experiment, the efflux of ^{14}C-PAH induced by 1mM PAH was monitored as a positive control of efflux.

Supplemental Figure 2.

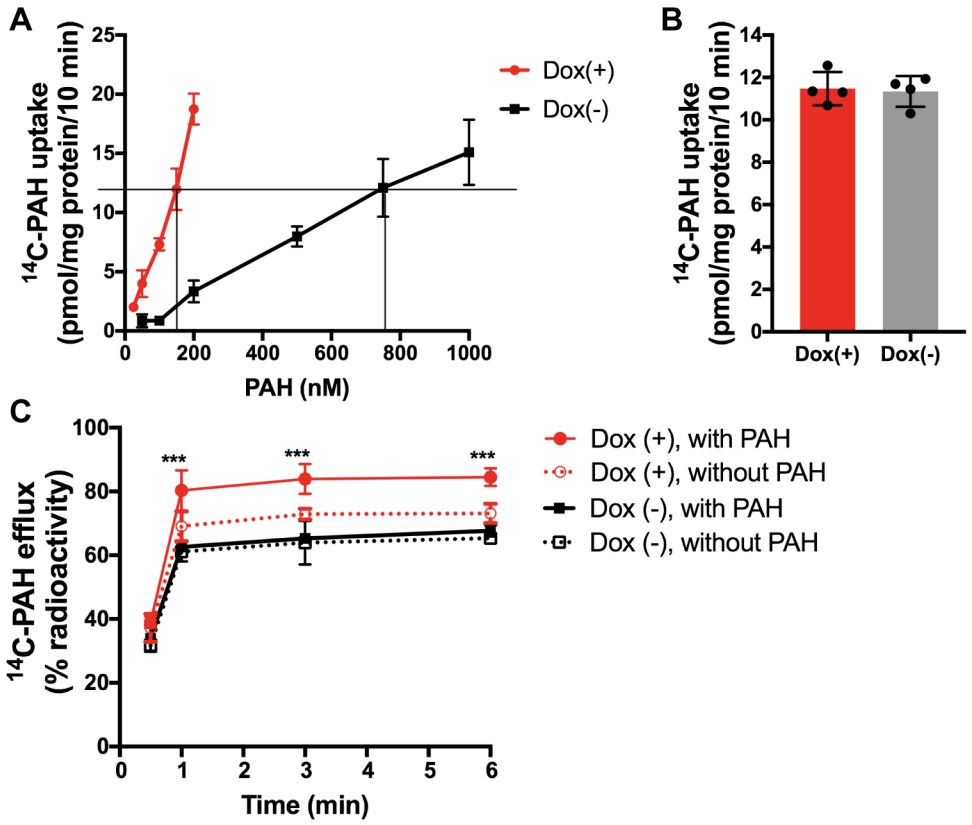

Supplemental Figure 2. Characterization of ^{14}C-PAH efflux mediated by OAT1. ***(A)*** To compare the efflux of ^{14}C-PAH in the presence or absence of OAT1 on the plasma membrane, we preloaded the same amount of ^{14}C-PAH to OAT1-expressing and non-expressing FlpIn293-TetR-hOAT1 cells, following the procedure described elsewhere (Shiraya et al., 2010). To preload the same amount ^{14}C-PAH, concentration dependence of the uptake of ^{14}C-PAH was determined for FlpIn293-TetR-hOAT1 cells with (+) or without (−) treatment with doxycycline ("Dox"). The uptake was measured for 10 min at the ^{14}C-PAH concentration of 25, 50, 100, 150, 200 nM for doxycycline-treated cells (Dox (+) shown in red), and 50, 100, 200, 500, 750, 1000 nM for the cells without doxycycline treatment (Dox (−) shown in black). To obtain equivalent loading of ^{14}C-PAH for both Dox (+) and Dox (−) cells, the concentration of ^{14}C-PAH was determined as 150 nM for Dox (+) cells and 750nM for Dox (−) cells, based on the results shown in ***(A)***. ***(B)*** The amount of ^{14}C-PAH loaded in Dox (+) and Dox (−) cells incubated for 10 min with ^{14}C-PAH at the concentration determined above, confirming the equivalent loading of ^{14}C-PAH. ***(C)*** Time course of the efflux of ^{14}C-PAH from Dox (+) and Dox (−) cells. Cells were preloaded with ^{14}C-PAH as described

above for the equivalent loading of ^{14}C-PAH. After washing with HBSS, the cells were incubated with or without of 100 μM non-radiolabeled PAH for 0.5, 1, 3, and 6 min. The radioactivity released from the cells was expressed as the percent of total preloaded radioactivity. *** $p < 0.001$: Dox (+) with PAH vs. Dox (+) without PAH at each timepoint. Data are expressed as means ± SD (n = 4). In Dox (+) cells, extracellularly applied PAH induced significant efflux of preloaded ^{14}C-PAH, whereas PAH did not induce significant efflux of ^{14}C-PAH in Dox (−) cells. Note that the concentration of PAH used for preloading in this experiment was lower than that used in the efflux experiments shown in the other figures, because, at higher concentration, it was difficult to obtain equivalent loading due to high transport activity of OAT1.

Supplemental Figure 3.

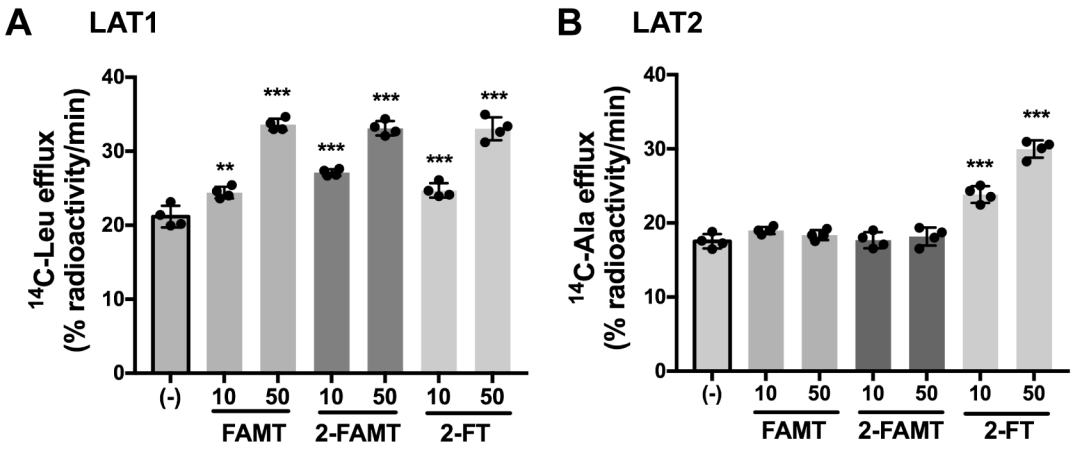

Supplemental Figure 3. Evaluation of the transport of FAMT, 2-FAMT, and 2-FT by amino acid transporters LAT1 and LAT2.

The transport of FAMT, 2-FAMT, and 2-FT by amino acid transporters LAT1 and LAT2 was examined by efflux experiments in which the efflux of preloaded ^{14}C-L-leucine and that of ^{14}C-L-alanine was measured in the cell line stably expressing human LAT1 (HEK293-LAT1 cells) ***(A)*** and human LAT2 (HEK293-LAT2 cells) ***(B)***, respectively (see "Supplemental Methods"). After pre-loading ^{14}C-L-leucine or ^{14}C-L-alanine and washing, the cells were incubated for 1 min in the presence or absence (−) of extracellularly applied compounds at the indicated concentration. The radioactivity in the medium regarded as the efflux was expressed as the percent of total preloaded radioactivity (see "Supplemental Methods"). ** $p = 0.0016$; *** $p < 0.001$ vs. (−). Data are expressed as means ± SD (n=4).

Supplemental Figure 4.

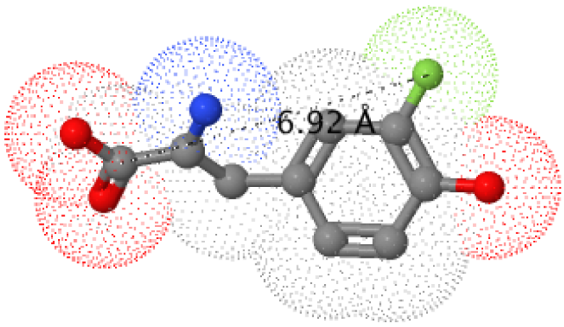

Supplemental Figure. 4 The 3D chemical structure model to measure the intramolecular distance.

The model is drawn by Jmol 14.6.4 (Jmol: an open-source Java viewer for chemical structures in 3D; http://jmol.org/). Atomic structures are shown in balls and sticks with dot surface. The compound is displayed at the front view. Carbon, nitrogen, oxygen, and fluorine atoms are shown in gray, blue, red and green, respectively. Hydrogen atoms are omitted in this display. The figure shows an example of the drawing of 3-FT. The distances (Å) from the carbonyl carbon of α-carboxyl group to the halogen groups at *ortho*-, *meta*-, and *para*-positions are listed as below. The distance of each compound was measured independently.

The distances from the carbonyl carbon of α-carboxyl group to the halogen groups at *ortho*-, *meta*-, and *para*-positions

Compound	distance (Å)
2-FT	4.45
2-IT	4.62
3-FT	6.92
3-IT	7.52
4-F-*m*-Tyr	7.94
4-I-*m*-Tyr	8.69

Supplemental Figure 5.

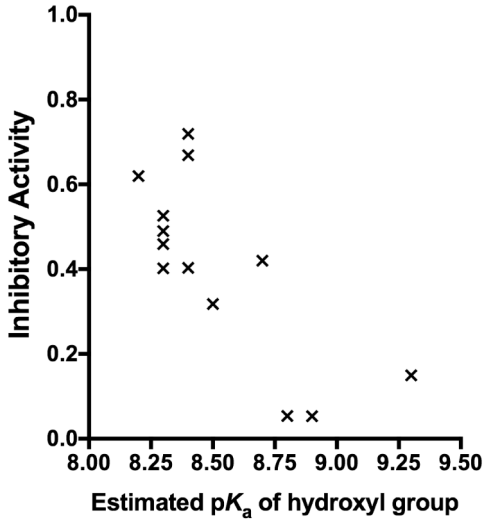

Supplemental Figure 5. The influence of pK_a of hydroxyl group on benzene ring on the inhibitory activity of the compounds.

The inhibitory activity of the compound is plotted against the estimated pK_a of hydroxyl group on the benzene ring among the fluorinated compounds. The inhibitory activity of each compound was measured at the concentration of 1mM and calculated following the equation: Inhibitory activity = 1− (Uptake expressed as % of control/100). Value 0 indicates "no inhibitory effect". Each point represents the mean value of 4 replicates for each compound. The estimated pK_a is listed in Table 1. The compounds included in the figure are FAMT, 3-FT, 2-FAMT, 2-FT, 2-F-*m*-Tyr, 4-F-*m*-Tyr, 5-F-*m*-Tyr, 6-F-*m*-Tyr, 3-F-*o*-Tyr, 4-F-*o*-Tyr, 5-F-*o*-Tyr, 6-F-*o*-Tyr, and AMT.

Supplemental Figure 6.

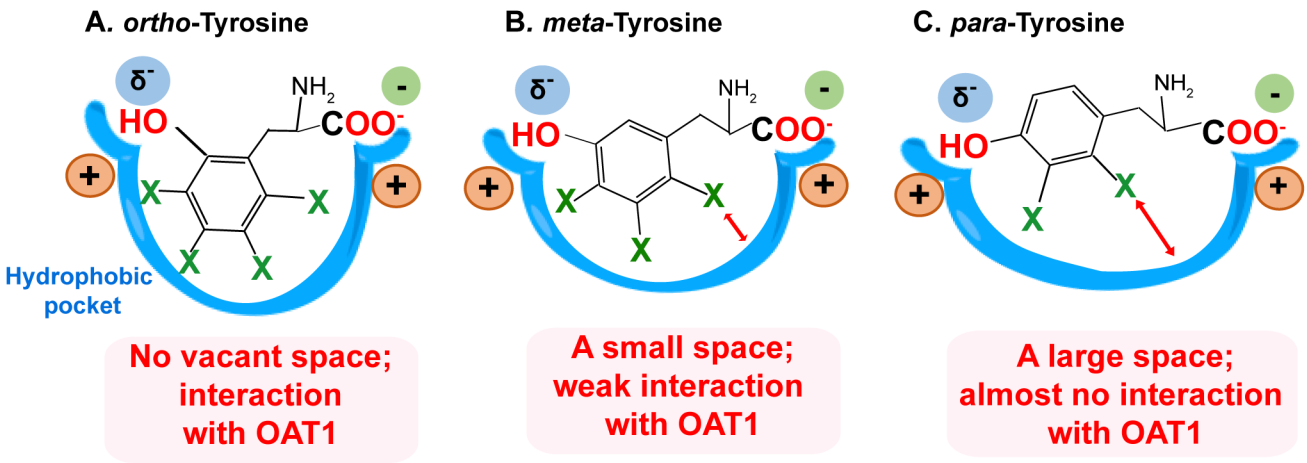

Supplemental Figure 6. Proposed binding models of fluorinated-tyrosine derivatives with OAT1.

The proposed binding models of fluorinated-tyrosine derivatives in the *ortho*-tyrosine ***(A)***, meta-tyrosine ***(B)*** and *para*-tyrosine ***(C)*** configurations. α-Carboxyl group binds with negative charge recognition site of OAT1, whereas the hydroxyl group that has a partial negative charge binds with the other negative charge recognition site. The negative charge recognition sites are located adjacent to the hydrophobic pocket of OAT1. In the *ortho*-tyrosine configuration ***(A)***, the hydrophobic core with any position of fluoro group may be accepted by the hydrophobic pocket of the OAT1. In the *meta*-tyrosine configuration ***(B)***, when the fluoro group is located at position 6 (6-F-*m*-Tyr), a vacant space may be formed between fluorine moiety and the bottom of hydrophobic pocket. The distance between fluorine moiety at position 2 and the bottom the hydrophobic pocket would be further increased in *para*-tyrosine configuration ***(C)***. This is an explanation why 2-FT exhibited almost no interaction with OAT1. "-X" in the figure represents a fluoro group.

Supplemental Figure 7.

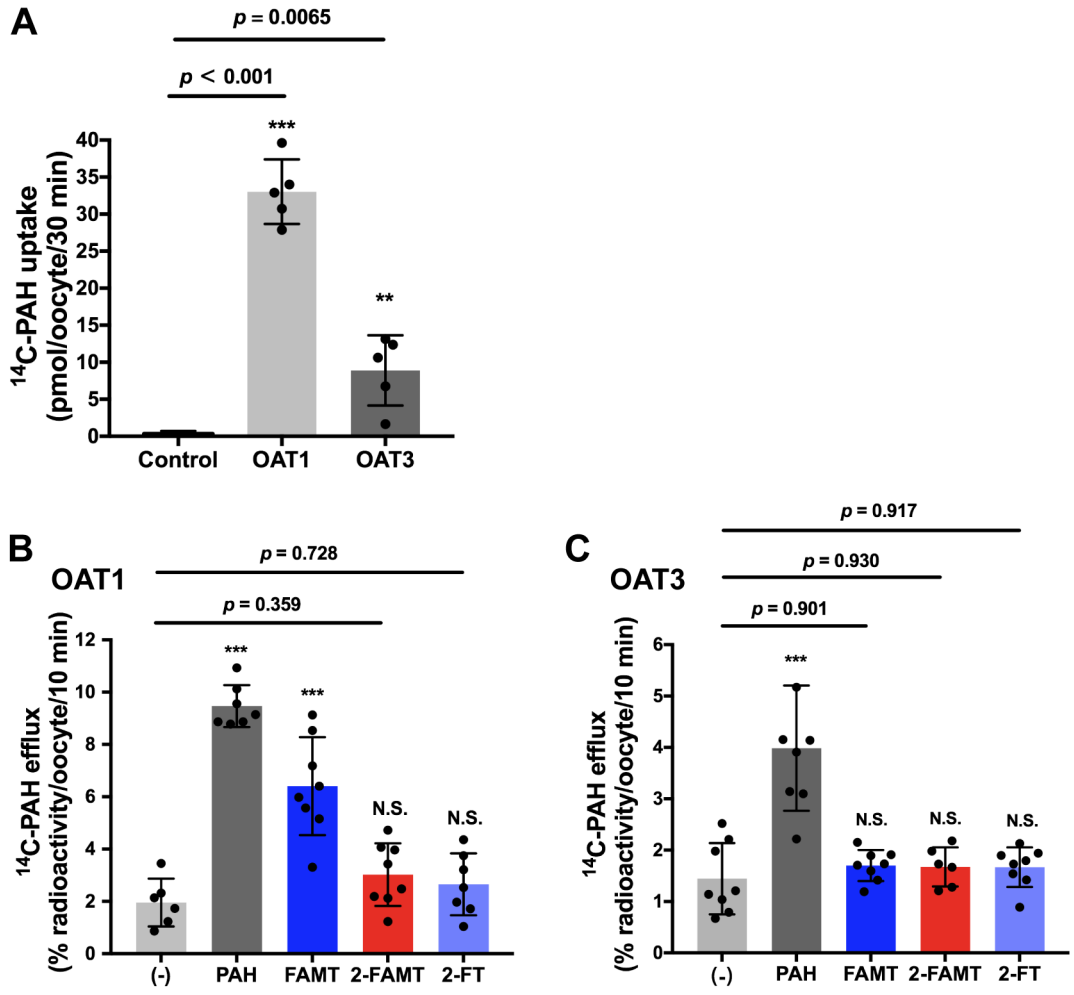

Supplemental Figure 7. Comparison of OAT1 and OAT3 in the transport of FAMT, 2-FAMT, and 2-FT.

For the comparison between OAT1 and OAT3, *Xenopus laevis* oocytes expressed with human OAT1 and human OAT3 were used following our previous study (Wei et al., 2016a). To evaluate the transport mediated by OAT1 and OAT3, efflux experiments were conducted taking advantage of their exchanger properties. After preloading with 50 μM ^{14}C-PAH, the oocytes were washed with Na^+-free ND96 solution, and incubated with test compounds. Then, the radioactivity in the medium and oocytes was measured. The preloading of oocytes with ^{14}C-PAH was confirmed by measuring the uptake of ^{14}C-PAH after the preloading ***(A)***. The high ^{14}C-PAH uptake was obtained for the oocytes expressing OAT1 and OAT3 compared with control oocytes without expressing OAT1 or OAT3. To examine the efflux of preloaded ^{14}C-PAH, the oocytes were incubated for 10 min in the presence or absence (−) of non-radiolabeled PAH, FAMT,

2-FAMT or 2-FT (500 μM). For both OAT1 and OAT3, extracellularly applied PAH induced higher efflux of preloaded ^{14}C-PAH than that without stimulation by the compounds (−), confirming their exchanger properties ***(B, C)***. In OAT1-expressing oocytes, FAMT induced the efflux of preloaded ^{14}C-PAH, whereas ^{14}C-PAH efflux was not induced by FAMT in OAT3-expressing oocytes. 2-FAMT and 2-FT did not induce significant ^{14}C-PAH efflux either for OAT1 or OAT3 ***(B, C)***. The efflux values were expressed as percentage of preloaded ^{14}C-PAH. $^{***}p < 0.001$ vs. (−). N.S., no significant difference compared with (−). Data are expressed as means ± SD (n = 6–8). The obtained results confirmed less transport of 2-FAMT and 2-FT by OAT1 compared with FAMT. The results, furthermore, suggest that FAMT, 2-FAMT and 2-FT are not transported by OAT3.